ELSEVIER

www.elsevier.nl/locate/jorganchem

Journal of Organometallic Chemistry 593–594 (2000) 392–402

Journal of Organometallic Chemistry

Solid state and solution structural studies of silver(I) cyclic complexes bearing the (Bzim)Ph_2P ligand

Fiorella Bachechi [a], Alfredo Burini [b,*], Rossana Galassi [b], Alceo Macchioni [c], Bianca Rosa Pietroni [b], Fabio Ziarelli [d], Cristiano Zuccaccia [c]

[a] *Istituto di Strutturistica Chimica 'G. Giacomello' CNR, Rome, Italy*
[b] *Dipartimento di Scienze Chimiche, Università, via S. Agostino 1, I-62032 Camerino, Italy*
[c] *Dipartimento di Chimica, Università, via Elce di Sotto 8, I-06123 Perugia, Italy*
[d] *ISRIM (Istituto Superiore di Ricerca e Formazione sui Materiali Speciali per le Tecnologie Avanzate), loc. Pentina Bassa 21, I-05100 Terni, Italy*

Received 8 July 1999; accepted 3 August 1999

Dedicated to Professor Fausto Calderazzo, an authentic nice person and a lighthouse for chemists.

Abstract

Cyclic silver(I) compounds having a $[\mu\text{-(Bzim)}Ph_2PAg]_2^{2+}$ unit ((Bzim)Ph_2P = 1-benzyl-2-imidazolyldiphenylphosphine) and NO_3^- (**I**), BF_4^- (**II**), and $B[3,5\text{-}(CF_3)_2C_6H_3]_4^-$ (**III**) as counterions were characterized in the solid state by X-ray crystal structure determinations (**I**, **II**), and in solution by ^{1}H-, ^{13}C-, ^{19}F- and ^{31}P-NMR spectroscopies. The crystal structure of complex $[\mu\text{-(Bzim)}Ph_2PAg(NO_3)]_n$ ($n = 2, 4$) (**I**) (triclinic, space group $P\bar{1}$ (no. 2), $a = 15.118(5)$, $b = 17.755(3)$, $c = 14.123(4)$ Å, $\alpha = 90.23(2)$, $\beta = 111.67(2)$, $\gamma = 85.92(2)°$, $Z = 2$) shows two conformers **A** and **B** in the unit cell. The conformer **A** consists of a tetranuclear species formed by two $[\mu\text{-(Bzim)}Ph_2PAg]_2^{2+}$ moieties, related by a center of symmetry, bonded together by two bridging nitrate anions. The nitrate anions are coordinated to the silver atoms in an unusual fashion. The conformer **B** is a dinuclear species where the silver atoms present in the eight-membered ring complete their tetracoordination with two chelate nitrate anions. The crystal structure of complex $\{[\mu\text{-(Bzim)}Ph_2PAg(BF_4)]_2\}_\infty$ (**II**) (monoclinic, space group $P2_1/c$ (no. 14), $a = 11.563(3)$, $b = 8.353(4)$, $c = 26.188(7)$ Å, $\beta = 95.88(2)°$, $Z = 2$) consists of infinite chains of the dinuclear cyclic silver moieties held together by BF_4^- bridging anions. The low temperature experimental and simulated ^{31}P-NMR spectra of complexes **I**–**III** show complex apparent doublets of multiplets due to the resonance of the spin systems of the three isotopomers of the silver atoms present in the cyclic units. The interionic solution structure of complex **II** was investigated by $^{19}F\{^1H\}$-HOESY NMR spectroscopy. In methylene chloride solution the BF_4^- anion is not more coordinated to the silver(I) atoms as in the solid state, and it is localized in between the phenyl and benzyl groups of the ligand.

Keywords: Silver complexes; Hybrid *P,N*-ligands; Coordinated NO_3^- and BF_4^- anions; Structure; ^{31}P- and $^{19}F\{^1H\}$-HOESY NMR spectroscopy

1. Introduction

Tertiary phosphines (R_3P) are important ligands in coordination chemistry because by changing the R groups it is possible to tune both the electronic and the steric properties of the ligand [1,2]. As far as silver(I)–phosphine derivatives are concerned a great deal of work has been done using monodentate phosphines and diphosphines [3]. The solid state of these classes of compounds is strongly influenced by the nature of the phosphine ligand coordinated to the silver ion, but an important role on the determination of the coordination number, geometry and nuclearity is also played by the counterion. In fact weakly coordinating anions, namely NO_3^- and ClO_4^- were found in the inner coordination sphere when PCy_3 was bonded to silver(I). Thus in $[Ag(PCy_3)_2NO_3]$ the silver ion results in being tetracoordinated while in $[Ag(PCy_3)_2ClO_4]$, it is tricoordinated [4]. However, bicoordinated $[L_2Ag]X$ has been structurally characterized (e.g. $[Ag\{P(CH_2CH_2CN)_3\}_2]$-

* Corresponding author. Tel.: +39-737-402243; fax: +39-737-637345.
E-mail address: burini@camserv.unicam.it (A. Burini)

0022-328X/00/$ - see front matter
PII: S0022-328X(99)00470-2

NO_3 [5], $[Ag\{P(mes)_3\}_2]PF_6$ (mes = $C_6H_2Me_3$-2,4,6)) [6]; in these examples the weakly coordinating anions results in the outer coordination sphere. When strongly coordinating anions such as Cl^- or Br^- were used, tetranuclear derivatives $[AgXPR_3]_4$ (R = Et or Ph) were isolated. In these compounds the halides are bridged to three metal atoms forming a cubane-like geometry [7,8]. Dinuclear cyclic silver derivatives are usually formed when diphosphine ligands are coordinated to silver(I), in these cases the counterion can be responsible of the ring conformations and of the nuclearity of the complex. In fact $[Ag_2(dpm)_2]^{2+}$ units (dpm = bis(-diphenylphosphino)methane) were isolated and structurally characterized in two conformations and having different nuclearity (e.g. $[Ag_2(dpm)_2(NO_3)_2]$ and $[Ag_4(dpm)_4(NO_3)_2]^{2+}$ [9]. Moreover a polymeric chain was found for $[Ag_2(dmpm)_2Br_2]$ (dmpm = bis(dimethylphosphine)methane) where the silver atoms of adjacent $[Ag_2(dmpm)_2]^{2+}$ units are linked by two Br^- anions [10].

While the behavior of silver–phosphine derivatives in the solid state has been well established, little has been done in solution [11–13]. Here we report an investigation in the solid state and in solution of cyclic silver(I) compounds **I**–**III** having a $[\mu\text{-(Bzim)}Ph_2PAg]_2^{2+}$ unit ((Bzim)Ph_2P

= 1-benzyl-2-imidazolyldiphenylphosphine) and NO_3^-, BF_4^-, and $B[3,5\text{-}(CF_3)_2C_6H_3]^{4-}$ as counterion (Scheme 1).

2. Results and discussion

Recently we reported the synthesis of dinuclear gold(I) and silver(I) complexes with the dihapto (Bzim)Ph_2P bridging phosphine ligand [14]. The incompletely resolved ^{31}P-NMR spectra of these silver(I) derivatives recorded in CD_3CN, left us to suppose a fluxional behaviour. On the other hand, ligand exchange equilibrium between cycles or isotopomers species [12] could occur in the same time. Thus, we decided to investigate in depth the actual nature of our silver complexes in the solid state and in solution. Particular effort was made in growing crystals suitable for X-ray crystal structure determinations. We had success when NO_3^- and BF_4^- were used as anions. Moreover in order to investigate the behavior of the compounds **I**–**III** in solution, low temperature 1D- and 2D-NMR characterization were performed.

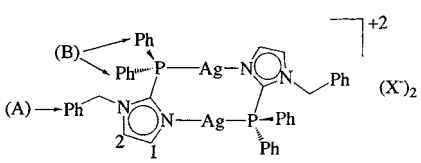

X^- = NO_3^- (**I**)
BF_4^- (**II**)
$B[3,5\text{-}(CF_3)_2(C_6H_3)]_4^-$ (**III**)

Scheme 1.

2.1. X-ray crystal structure analyses of *I* and *II*

Single crystals of the compound **I** suitable for an X-ray structure determination were obtained from an acetonitrile–ethyl ether solution while crystals of **II** grew from a dichloromethane–hexane solution. X-ray diffraction effects of single crystals of the two complexes were collected on a Rigaku AFC5R diffractometer using graphite monochromated Cu–K_α radiation and a 12 kV rotating anode generator. Intensity data were collected by ω–2θ technique to a maximum 2θ value of about 124°. The structures were solved by Patterson and subsequent Fourier syntheses and refined by full-matrix least-squares method with anisotropic thermal parameters for all non-hydrogen atoms for **II**. For complex **I** the carbon atoms of the phenyl groups and of the solvent were refined isotropically. The hydrogen atoms were included at calculated positions and not refined. Crystal parameters and structure determination data for **I** and **II** are given in Table 1. Atomic scattering factors and anomalous dispersion terms were taken from the International Tables [15]. All calculations were performed using the TEXAN crystallographic software package [16]. The asymmetric unit of **I** (Fig. 1) contains one molecule of the binuclear complex with the connected counterions and one-half of another independent molecule with a counterion, related by a center of symmetry to its other half and counterion. Also a molecule of ethyl ether was found included. The asymmetric unit of **II** (Fig. 4) contains only half a molecule of the binuclear complex with the coordinated counterion and one molecule of solvent (CH_2Cl_2) and it is completed by a center of symmetry. Final atomic coordinates are listed in Table 2 for **I** and Table 4 for **II**.

2.2. Molecular structure of $[\mu\text{-(Bzim)}Ph_2PAg(NO_3)]_n$ (n = 2, 4) (*I*)

The crystal structure of $[\mu\text{-(Bzim)}Ph_2PAg(NO_3)]_n$ (**I**), is particularly interesting. The unit cell of the complex shown in Fig. 1 consists of two independent molecules (**A** with $n = 4$ and **B** with $n = 2$) and a selection of bonds distances and angles are listed in Table 3. **A** and **B** coexist with different conformations of the eight-membered cycle. Moreover, depending on different coordinative fashions of the nitrate anions, dinuclear and tetranuclear species were observed. Two molecules of type **A** (Fig. 2), related by a center of symmetry, are bound together by two bridging nitrate anions to form

Table 1
Crystallographic data for **I** and **II**

Compound	**I**	**II**
Empirical formula	$C_{71}H_{69}N_9O_9P_3Ag_3$	$C_{46}H_{42}N_4B_2F_8P_2Cl_4Ag_2$
Formula weight	1608.92	621.98
Crystal size (mm)	$0.15\times0.30\times0.50$	$0.03\times0.07\times0.40$
Crystal system	Triclinic	Monoclinic
a (Å)	15.118(5)	11.563(3)
b (Å)	17.755(3)	8.353(4)
c (Å)	14.123(4)	26.188(7)
α (°)	90.23(2)	
β (°)	111.67(2)	95.88(2)
γ (°)	85.92(2)	
V (Å^3)	3513(3)	2516(2)
Space group	$P\bar{1}$ (no. 2)	$P2_1/c$ (no. 14)
Z	2	2
D_{calc} (g cm^{-3})	1.522	1.628
$F(000)$	1632	1230
μ(Cu–K$_\alpha$) (cm^{-1})	79.43	95.27
Diffractometer	Rigaku AFC5R	Rigaku AFC5R
Scan type	ω–2θ	ω–2θ
Scan rate (° min^{-1})	32.00 (3 rescans)	8.0 (3 rescans)
Scan width (°)	$1.52+0.30\tan\theta$	$0.94+0.30\tan\theta$
2θ Max. (°)	123.9	124.10
Total measured reflections	11513	4522
Unique measured reflections	11039 ($R_{int}=0.026$)	4287 ($R_{int}=0.054$)
Corrections	Lorentz polarization absorption	Lorentz polarization absorption
Transmission factor	0.75–1.00	0.67–1.00
Structure solution	Patterson method	Patterson method
Refinement	Full-matrix least-squares	Full-matrix least-squares
Function minimized	$\Sigma w(\|F_o\|-\|F_c\|)^2$	$\Sigma w(\|F_o\|-\|F_c\|)^2$
Least-squares weights	$4\ F_o^2/\sigma^2(F_o^2)$	$4\ F_o^2/\sigma^2(F_o^2)$
p-Factor	0.03	0.03
Observed reflections	7731 [$I>3.00\sigma(I)$]	2651 [$I>3.00\sigma(I)$]
Variables	408	316
Reflections/parameters	20.15	8.39
R, R_w	0.076, 0.096	0.052, 0.069
Goodness-of-fit	2.50	1.78
Max. shift/error	0.05	0.05
Max. peak difference map (e Å^{-3})	0.88	0.60
Min. peak difference map (e Å^{-3})	−0.65	−0.54

tetranuclear aggregates. It should be underlined the unusual coordination mode of the nitrate anions [17] (Fig. 3a). In fact they form interannular bridges by the O(3) and O(3′) atoms (Ag(1)–O(3) 2.40(1) Å and Ag(1)–O(3′) 2.53(1) Å), at the same time they form intraannular bridges using O(1) and the related O(1′) (Ag(2)–O(1) 2.66(1) Å). The other two nitrate anions, present in the structure of **A**, are chelated to the external Ag(2) silver atoms (Ag(2)–O(4) 2.52(1) Å; Ag(2)–O(6) 2.71(1) Å). The Ag–O distances are in the same range of that found in $Ag_2(NO_3)_2(m\text{-PP})_2$ (m - PP = 1,3 - bis[(diphenylphosphino)methyl]benzene) where the bridging nitrate anions are coordinated to the silver atoms through a single O atom [18]. The frame of each cycle is constituted by eight atoms where the silver ones are 2.97(2) Å apart. There is an extensive discussion over a bonding distance between atoms in a d^{10}–d^{10} closed shell [19,20], thus in compound **I** the Ag–Ag distance is not indicative of a metal–metal interaction, because the sum of the metallic radii of two Ag atoms is 2.884 Å [21]. In contrast the hexameric cluster $\{[Ag(Im)_2][ClO4]\}_6$ (Im = imidazole) is held primarily by Ag···Ag interactions with metal–metal distances in the range 3.051–3.493 Å [22]. In complex **I** the coordination around the silver atoms are completed by the phosphorous and nitrogen atoms of two head-to-tail (Bzim)Ph_2P phosphine bridging ligands. In this way Ag(1) resulted in tetracoordinated while Ag(2) resulted in pentacoordinated. Ag(1)–P(1) and Ag(2)–P(2) distances are 2.368(3) and 2.397(3) Å, respectively while Ag(1)–N(1) and Ag(2)–N(3) distances are 2.247(3) and 2.215(3) Å, respectively. Comparable coordination bond distances were also reported in related complexes $[Ag_2(\mu\text{-ppye})]^{2+}$ (ppye = 1-(diphenylphosphino)-2-(2-pyridyl)ethane) [23], $[Ag_2Cl_2(pyPh_2P)_3]$ ($pyPh_2P$ = diphenylpyridylphosphine) [24], $[Ag_4(dpm)_4(NO_3)_2]^{2+}$ [9], $[Ag_2(\eta^1\text{-dppy})(\mu\text{-dppy})_2][ClO_4]_2$ [25] and in a pyrazolate–phosphine silver derivative $[Ag_2(pz)_2(PPh_3)_2]$ [26].

The solid-state structure of molecule **B**, which has crystallographic C_2 symmetry (Fig. 2), consists of a neutral dinuclear unit with the two silver atoms bridged by a pair of (Bzim)Ph_2P ligands forming an eight-mem-

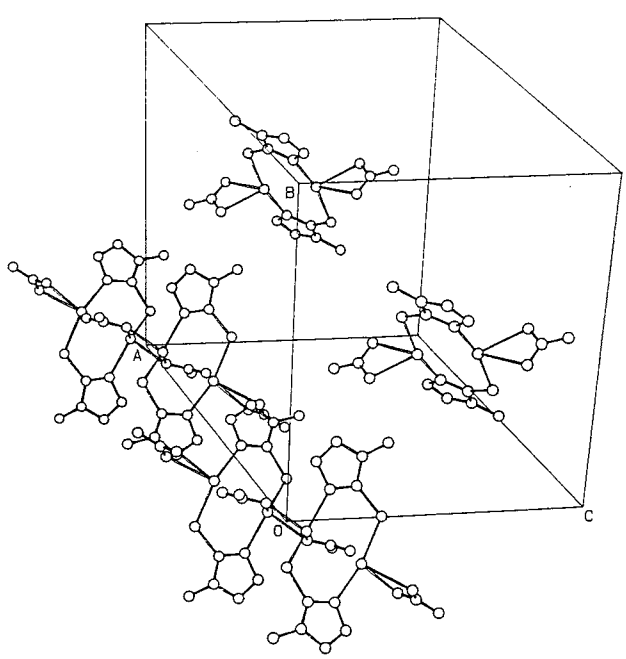

Fig. 1. Unit cell content of **I** showing a row of molecules of type **A** joined to form tetramers and a row of isolated molecules of type **B**.

Table 2
Atomic coordinates and equivalent isotropic thermal parameters of complex **I** with estimated S.D. values in parentheses

	x/a	y/h	z/c	B_{eq}
Ag(1)	0.87639(6))	0.04527(6	0.00022(7)	4.42(4)
Ag(2)	0.76715(7)	0.00477(5)	0.12716(7)	4.41(4)
Ag(3)	0.05926(6)	0.46931(4)	0.43941(7)	3.86(4)
P(1)	0.7306(2)	0.0304(2)	−0.1375(2)	3.6(1)
P(2)	0.8222(2)	0.1177(2)	0.2166(2)	3.4(1)
P(3)	0.0374(2)	0.5938(2)	0.3683(2)	3.4(1)
O(1)	0.9403(9)	−0.0664(7)	0.185(1)	8.6(3)
O(2)	1.0644(9)	−0.1354(7)	0.192(1)	8.7(3)
O(3)	0.9915(7)	−0.0584(6)	0.0661(8)	6.2(2)
O(4)	0.7642(9)	−0.0944(7)	0.253(1)	5.8(3)
O(5)	0.6732(8)	−0.1049(6)	0.3377(8)	7.3(3)
O(6)	0.6526(8)	−0.0110(6)	0.2341(8)	7.1(2)
O(7)	0.0744(7)	0.3943(6)	0.2952(7)	6.3(2)
O(8)	0.1834(9)	0.3659(7)	0.236(1)	8.4(3)
O(9)	0.2184(8)	0.4185(6)	0.3819(8)	7.0(2)
N(1)	0.9258(7)	0.1454(5)	0.0986(7)	4.2(4)
N(2)	0.9321(7)	0.2399(5)	0.2043(7)	4.0(4)
N(3)	0.6680(7)	−0.0470(6)	−0.0112(7)	4.3(4)
N(4)	0.5707(6)	−0.0594(5)	−0.1697(7)	3.9(4)
N(5)	0.0915(6)	0.3695(5)	0.5402(7)	3.4(4)
N(6)	−0.1081(7)	0.7154(5)	0.3410(7)	3.7(4)
N(7)	1.0019(8)	−0.0852(6)	0.1520(8)	4.9(2)
N(8)	0.6952(7)	−0.0713(6)	0.2738(8)	4.1(2)
N(9)	0.1596(8)	0.3934(7)	0.303(1)	5.3(2)
C(1)	0.8976(8)	0.1705(6)	0.1714(8)	3.3(2)
C(2)	0.986(1)	0.2560(8)	0.147(1)	5.1(3)
C(3)	0.982(1)	0.1995(7)	0.080(1)	4.8(3)
C(4)	0.9194(9)	0.2862(7)	0.281(1)	4.4(2)
C(5)	0.6524(8)	−0.0300(6)	−0.1074(8)	3.5(2)
C(6)	0.534(1)	−0.0981(8)	−0.110(1)	5.1(3)
C(7)	0.596(1)	−0.0903(8)	−0.010(1)	4.9(3)
C(8)	0.5261(8)	−0.0520(7)	−0.2818(9)	4.1(2)
C(9)	0.848(1)	0.3535(7)	0.242(1)	4.6(3)
C(10)	0.794(1)	0.3672(9)	0.140(1)	6.2(3)
C(11)	0.722(1)	0.432(1)	0.110(2)	8.4(5)
C(12)	0.714(1)	0.477(1)	0.188(1)	8.0(4)
C(13)	0.766(1)	0.463(1)	0.286(1)	7.6(4)
C(14)	0.837(1)	0.400(1)	0.315(1)	6.2(3)
C(15)	0.5463(8)	−0.1218(6)	−0.3370(9)	3.7(2)
C(16)	0.516(1)	−0.1135(9)	−0.441(1)	6.2(3)
C(17)	0.535(1)	−0.176(1)	−0.499(1)	7.0(4)
C(18)	0.578(1)	−0.239(1)	−0.451(1)	7.2(4)
C(19)	0.612(1)	−0.250(1)	−0.345(1)	7.6(4)
C(20)	0.592(1)	−0.1877(9)	−0.286(1)	6.1(3)
C(21)	0.7195(8)	0.1868(6)	0.1959(8)	3.6(2)
C(22)	0.701(1)	0.2241(7)	0.275(1)	4.7(3)
C(23)	0.622(1)	0.2768(9)	0.250(1)	6.3(3)
C(24)	0.565(1)	0.295(1)	0.148(1)	6.6(4)
C(25)	0.583(1)	0.257(1)	0.072(1)	6.3(3)
C(26)	0.662(1)	0.2032(7)	0.093(1)	4.9(3)
C(27)	0.8876(7)	0.1075(6)	0.3531(8)	3.3(2)
C(28)	0.9855(9)	0.1188(7)	0.396(1)	4.3(2)
C(29)	1.0355(9)	0.1082(7)	0.500(1)	4.5(2)
C(30)	0.989(1)	0.0851(7)	0.563(1)	4.8(3)
C(31)	0.894(1)	0.0704(8)	0.520(1)	5.2(3)
C(32)	0.8417(8)	0.0805(7)	0.4138(9)	4.1(2)
C(33)	0.6617(9)	0.1208(7)	−0.178(1)	4.3(2)
C(34)	0.568(1)	0.1331(8)	−0.187(1)	5.1(3)
C(35)	0.521(1)	0.208(1)	−0.212(1)	7.2(4)
C(36)	0.573(1)	0.264(1)	−0.225(1)	7.6(4)
C(37)	0.663(1)	0.253(1)	−0.216(1)	8.4(5)
C(38)	0.717(1)	0.178(1)	−0.190(1)	7.8(4)
C(39)	0.7428(8)	−0.0134(7)	−0.250(1)	4.2(2)
C(40)	0.704(1)	0.0202(8)	−0.347(1)	5.0(3)
C(41)	0.715(1)	−0.024(1)	−0.428(1)	7.0(4)
C(42)	0.763(1)	−0.095(1)	−0.409(1)	7.1(4)
C(43)	0.805(1)	−0.124(1)	−0.315(1)	7.1(4)
C(44)	0.797(1)	−0.0827(9)	−0.229(1)	6.0(3)
C(45)	−0.0588(8)	0.6505(6)	0.3875(8)	3.4(2)
C(46)	0.1751(9)	0.2636(7)	0.618(1)	4.6(2)
C(47)	0.1620(9)	0.3168(7)	0.542(1)	4.3(2)
C(48)	−0.1009(8)	0.7565(7)	0.2522(9)	3.9(2)
C(49)	−0.1708(9)	0.7338(7)	0.152(1)	4.3(2)
C(50)	−0.248(1)	0.6910(9)	0.141(1)	6.1(3)
C(51)	−0.315(1)	0.673(1)	0.043(1)	7.2(4)
C(52)	−0.299(1)	0.698(1)	−0.042(1)	7.5(4)
C(53)	−0.224(1)	0.740(1)	−0.034(1)	6.8(4)
C(54)	−0.161(1)	0.7587(8)	0.064(1)	5.9(3)
C(55)	0.0099(8)	0.5939(7)	0.2312(9)	3.9(2)
C(56)	0.061(1)	0.6326(8)	0.186(1)	5.1(3)
C(57)	0.036(1)	0.6286(8)	0.080(1)	6.0(3)
C(58)	−0.037(1)	0.588(1)	0.023(1)	6.6(4)
C(59)	−0.090(1)	0.548(1)	0.067(1)	6.7(4)
C(60)	−0.067(1)	0.5505(8)	0.171(1)	5.1(3)
C(61)	0.1453(8)	0.6458(6)	0.4175(8)	3.6(2)
C(62)	0.230(1)	0.6037(8)	0.436(1)	5.1(3)
C(63)	0.315(1)	0.640(1)	0.463(1)	7.2(4)
C(64)	0.314(1)	0.718(1)	0.467(1)	6.2(3)
C(65)	0.227(1)	0.7580(9)	0.449(1)	5.8(3)
C(66)	0.1416(9)	0.7238(7)	0.425(1)	4.5(2)
C(79)	0.404(2)	0.430(2)	0.606(2)	16.1(8)
C(80)	0.473(2)	0.491(2)	0.648(2)	16.9(9)
C(81)	0.553(1)	0.463(1)	0.715(2)	8.6(5)
C(82)	0.620(2)	0.516(2)	0.750(2)	16.3(9)
C(83)	0.707(2)	0.480(2)	0.818(2)	13.6(8)

bered ring. In addition, each silver atom completes its tetracoordination with a chelate nitrate anion. The Ag–P and Ag–N bond distances are in the same range of those observed in molecule **A**. The nitrate anion is asymmetrically bonded to the silver atom, Ag(3)–O(7) is 2.51(1) and Ag(3)–O(9) is 2.90(1) Å; these distances are slightly longer than those observed in the related $[Ag_2(dpm)_2(NO_3)_2]$ [9] and $[Ph_3PAgNO_3]$ [27] compounds. Also in molecule **B** the Ag(3)···Ag(3′) separation of 3.048(2) is indicative of a nonbonding interaction. As already underlined the cycles **A** and **B** have different folded conformations along the Ag–Ag axis with P–Ag–N fragments eclipsed in **A** and staggered in **B** (Fig. 3b). The P(1)–Ag(1)–N(1) angle is 130.8(2) and P(2)–Ag(2)–N(3) angle is 147.7(2)° (molecule **A**) while the P(3)–Ag(3)–N(5) angle is 165.9(2)° (molecule **B**).

2.3. Molecular structure of $\{[\mu\text{-}(Bzim)Ph_2PAg(BF_4)]_2\}_\infty$ (II)

Atomic coordinates for compound **II** are listed in Table 4 and selected bonds and angles are listed in Table 5.

As in compound **I**, one of the most interesting features of the crystal structure of **II** is the non innocent role of the counterion. In fact BF_4^- is usually considered a weak coordinating anion but the centrosymmetric molecular structure of $[\mu\text{-}(Bzim)Ph_2PAg(BF_4)]_2$ consists of infinite chains of the dinuclear cyclic silver moieties held together by BF_4^- bridging anions (Fig. 4), with Ag(1)–F(1) and Ag(1)–F(3″) distances of 2.779(8) and 2.756(6) Å, respectively. These distances are shorter of that found in $Ag(TMB)BF_4$ (TMB = 2,5-dimethyl-2,5-diisocyanohexane) (Ag–F = 2.873(6) Å) [28]. Few other examples where the BF_4^- anions behave as a bidentate bridging ligand are reported in the literature [29,30]. The unusual coordination modes of the tetrafluoroborate anions result in the formation of staggered eight membered cycles that lie in an almost perpendicular plane respect to those of the dinuclear silver–phosphine rings. The coordination of two BF_4^- anions for each silver atom means that the $(Bzim)Ph_2P$ ligands do not give enough electron density to stabilize the metal centers.

Even in compound **II** the dinuclear cycle is formed by two head-to-tail $(Bzim)Ph_2P$ ligands coordinated to two silver atoms (Fig. 5). In this case the conformation of the $[\mu\text{-}((Bzim)Ph_2P)_2Ag_2]^{2+}$ ring is almost planar with an angle N(1)–Ag(1)–P(1) of 172.7(2)°. The silver atom results tetracoordinated and the Ag(1)···Ag(1′) distance of 2.910(2) Å is the shortest distance when compared with those found in compound **I**. While the Ag(1)–P(1) bond length (2.361(2) Å) is in the range of those found in **I**, the Ag(1)–N(1) distance (2.148(7) Å) is relatively shorter than those found in the analogous-nitrate derivative **I**. This is more evidence that the absence of a nitrate group coordinated to the silver atom improves its Lewis acidity.

In conclusion, we observed that in the solid state, the $[\mu\text{-}(Bzim)Ph_2P)_2Ag_2]^{2+}$ moiety results in coordination to the counterions even if these are considered weakly coordinating.

Table 3
Selected bond distances (Å) and angles (°) of complex **I**

Molecule **A**			
Coordination sphere around Ag(1)		Coordination sphere around Ag(2)	
Ag(1)···Ag(2)	2.970(2)	Ag(2)–P(2)	2.397(3)
Ag(1)···Ag(1′)	3.966(2)	Ag(2)–N(3)	2.215(3)
Ag(1)–P(1)	2.368(3)	Ag(2)–O(1)	2.66(1)
Ag(1)–N(1)	2.247(3)	Ag(2)–O(4)	2.52(1)
Ag(1)–O(3)	2.40(1)	Ag(2)–O(6)	2.71(1)
Ag(1)–O(3′)	2.53(1)	Ag(1)···Ag(2)–P(2)	84.94(9)
Ag(2)···Ag(1)–P(1)	83.84(9)	Ag(1)···Ag(2)–N(3)	86.7(3)
Ag(2)···Ag(1)–N(1)	89.3(3)	Ag(1)···Ag(2)–O(4)	141.7(2)
Ag(2)···Ag(1)–O(3)	92.3(3)	P(2)–Ag(2)–N(3)	147.7(2)
Ag(2)···Ag(1)–O(3′)	163.07(4)	P(2)–Ag(2)–O(1)	94.5(2)
Ag(1)–O(3)–Ag(1′)	107.1(4)	P(2)–Ag(2)–O(4)	109.5(2)
P(1)–Ag(1)–N(1)	130.8(2)	P(2)–Ag(2)–O(6)	90.0(2)
P(1)–Ag(1)–O(3)	121.3(2)	N(3)–Ag(2)–O(1)	110.4(3)
P(1)–Ag(1)–O(3′)	109.5(2)	N(3)–Ag(2)–O(4)	96.2(3)
N(1)–Ag(1)–O(3)	107.6(3)	N(3)–Ag(2)–O(6)	93.5(3)
N(1)–Ag(1)–O(3′)	88.8(4)	O(1)–Ag(2)–O(4)	76.7(4)
O(3)–Ag(1)–O(3′)	72.9(4)	O(1)–Ag(2)–O(6)	121.3(4)
		O(4)–Ag(2)–O(6)	47.2(4)

Molecule **B**	
Coordination sphere around Ag(3)	
Ag(3)···Ag(3′)	3.048(2)
Ag(3)–P(3)	2.379(3)
Ag(3)–N(5)	2.190(3)
Ag(3)–O(7)	2.51(1)
Ag(3)–O(9)	2.90(1)
Ag(3′)···Ag(3)–P(3)	86.05(9)
Ag(3′)···Ag(3)–N(5)	85.3(3)
Ag(3′)···Ag(3)–O(7)	150.6(2)
Ag(3′)···Ag(3)–O(9)	162.6(2)
P(3)–Ag(3)–N(5)	165.9(2)
P(3)–Ag(3)–O(7)	100.2(2)
P(3)–Ag(3)–O(9)	96.5(2)
N(5)–Ag(3)–O(7)	92.8(3)
N(5)–Ag(3)–O(9)	88.4(3)
O(7)–Ag(3)–O(9)	46.0(2)

2.4. NMR spectroscopy

2.4.1. Intramolecular characterization

Complexes **I**–**III** were characterized in solution by ^{1}H-, ^{13}C-, ^{19}F- and ^{31}P-NMR spectroscopies. The assignment of all the ^{1}H and ^{13}C resonances of complex **II** carried out at 217 K is discussed in detail because it is the only one where the complex $[\mu\text{-}(Bzim)Ph_2P)_3Ag_2X_2]$ is almost completely absent.

^{1}H- and ^{13}C-NMR. The resonances of the aromatic rings were easily assigned starting from the *ortho*-protons that appear as doublet for the (A) ring and doublet of doublet for the (B) rings (due to the additional coupling constant with ^{31}P). The other aromatic resonances were assigned based on the scalar connectivity evidenced by the ^{1}H-COSY NMR spectra. The CH_2 protons were assigned because they are the most shielded of the molecule. The distinction between the remaining two singlets due to the Im-protons (Im = imidazole ring) was achieved by the observation of a NOE contact in the ^{1}H-NOESY NMR spectrum between H-2 and CH_2 protons. The ^{13}C resonances were assigned by recording ^{1}H{^{13}C}-COSY NMR spectra 'standard' and long range.

^{31}P-NMR. The spectra of complexes **I**–**III** appear as two broad resonances at room temperature (302 K) that sharpened into quite complicated apparent doublets of multiplets (Fig. 6) on lowering the temperature. These were simulated [31] as due to the superimposition of the resonances of the spin systems of the three isotopomers $^{107}Ag^{109}Ag^{31}P^{31}P'$ (50.0%), $^{107}Ag^{107}Ag'^{31}$-

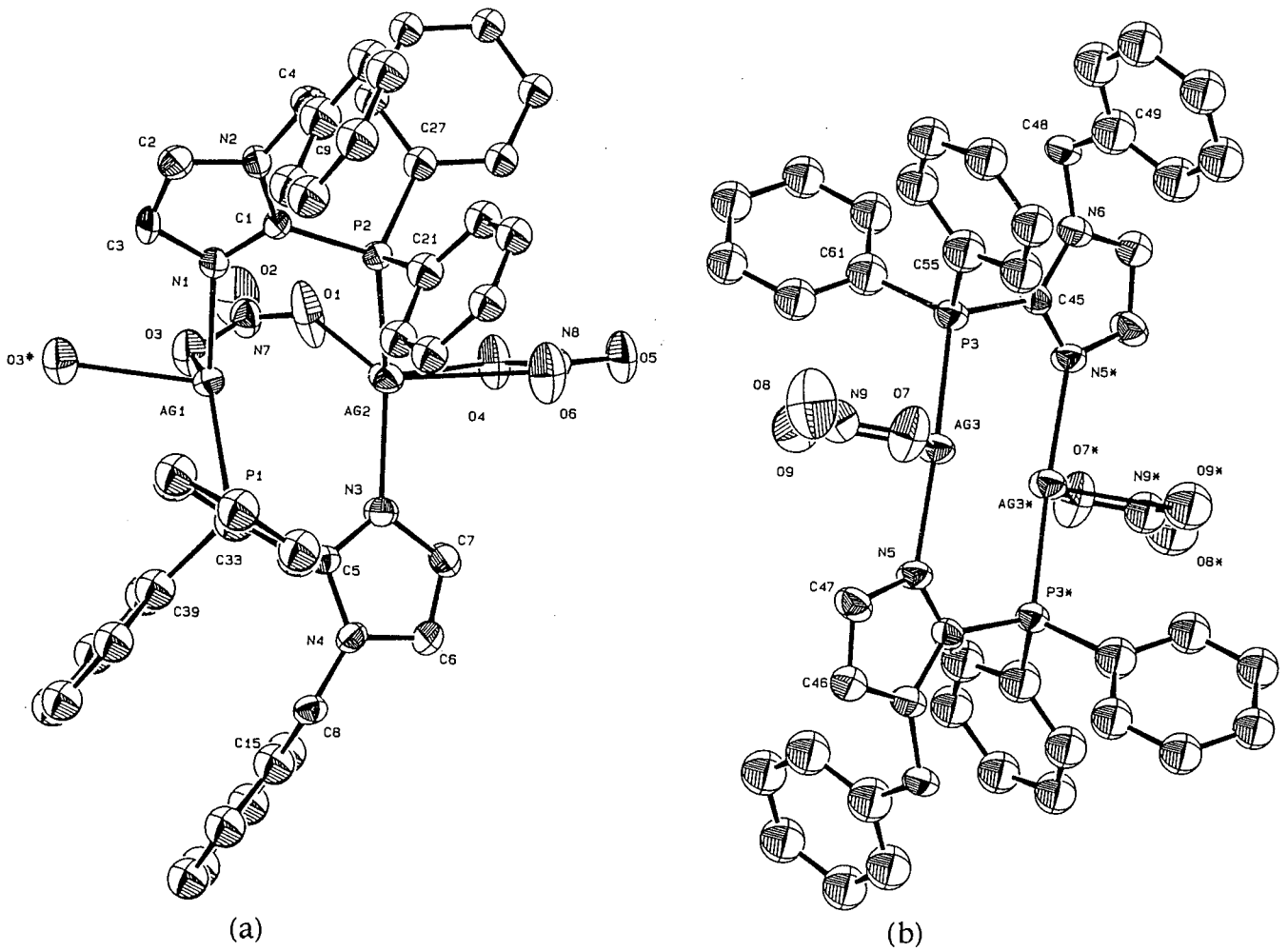

Fig. 2. ORTEP plot of **I** with the numbering schemes of the atoms. (a) Molecule **A** and (b) molecule **B**, atoms labeled with asterisks are centrosymmetric. Thermal ellipsoids are shown at 40% probability levels.

$P^{31}P'$ (25.9%) and $^{109}Ag'^{109}Ag^{31}P^{31}P'$ (24.1%) where all the coupling constants are not equal to zero with the exception of ^4J(Ag–Ag). The experimental and simulated ^{31}P-NMR spectra of complexes **II** recorded at 217 K are shown in Fig. 7. The NMR parameters obtained by the simulations are reported in Table 6 and they are little affected by the nature of the counterion. This indicates that in solution the counterions weakly interact with the metallic centers. On the other hand, there must be a weak interaction because the trends both in chemical shifts and in coupling constants are just what one expects based on the coordinating capability of the counterions. By decreasing the coordinating capability of the counterions, in fact, the ^{31}P chemical shift increases (less shielded phosphorous) and the $^1J(^{31}P–^{107/9}Ag)$ coupling constants slightly increase. The ratio of the $^nJ(^{31}P–^{107}Ag)/^nJ(^{31}P–^{109}Ag)$ ($n = 1$ and 3) coupling constants that come out from the simulations is close to the theoretical value caused by the gyromagnetic ratio of the two silver isotopes (1.15). The $^1J(^{31}P–^{107/9}Ag)$ coupling constants are quite large for a silver di-coordinated [32] as observed by Van Koten and coworkers [33] but very close to those reported by Del Zotto et al. [23] for similar compounds. The $^3J(^{31}P–^{107/9}Ag)$ coupling constants have the opposite sign of $^1J(^{31}P–^{107/9}Ag)$ and are substantially larger than those observed for similar compounds [33]. It is interesting to note that also the $^4J(^{31}P–^{31}P)$ are quite large, too.

2.5. Interionic interactions in solution

The cation–anion relative position [34–38] for complex **II** was investigated by $^{19}F\{^1H\}$-HOESY NMR spectroscopy in methylene chloride solution. At 217 K the dynamic processes are frozen enough to allow the localization of the counterion with respect to the cationic moiety. Interionic contacts were observed between the fluorine atoms of BF_4^- and the *ortho* (very strong) *meta* and/or *para* (medium) aromatic protons of the phosphine ligand and the *ortho* protons of the benzyl group (weak) (see Fig. 8). No interionic contact

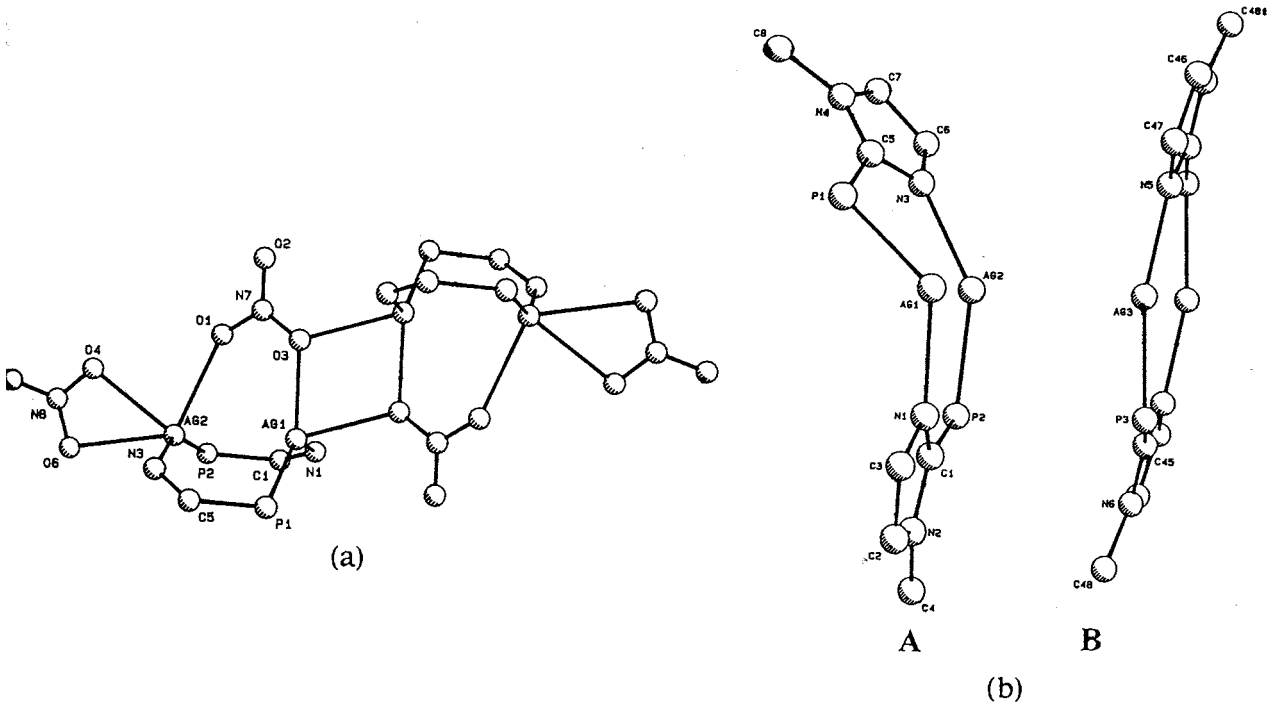

Fig. 3. (a) The core of $[\mu\text{-(Bzim)}Ph_2PAg(NO_3)]_4$ (**I**), showing the unusual coordination mode of the nitrate anions and the formation of tetramers by a center of symmetry. (b) The cores of molecules **A** and **B** of **I** showing the different conformations of the eight-membered rings.

was observed between the counterion and Im- and CH_2-protons. Furthermore, a strong interionic contact was also observed between the counterion and a very small proton resonance at 2.13 ppm probably due to water.

The results reported above indicate that the counterion interacts only with the protons that comes out from the eight-membered plane formed by $[\mu\text{-(Bzim)}Ph_2P)_2Ag_2]^{2+}$ moiety atoms and, in particular, with the phosphino phenyl groups. Therefore, it must stay above or below the cycle a little shifted towards the phosphorous atom. It is interesting to note that the solution interionic structure of **II** differs from the solid state where the counterions are located between two eight-membered planes but are clearly close to the Im-protons. In contrast, in solution we do not observe interionic contacts between such protons and the counterion. It is not surprising that the solution and solid state interionic structures differ [39] because the interaction energies are so low that the packing forces and the solvent interactions can easily afford a different minimum of potential energy for the counterion.

3. Conclusion

In the study reported here, we point out the important role played by the counterions present in $[\mu\text{-(Bzim)}Ph_2PAg]_2^{2+}$ complexes. In the solid state the NO_3^- and BF_4^- anions yield dinuclear, tetranuclear and polynuclear silver(I) cyclic complexes having different conformations. Moreover unusual coordination modes of the anions NO_3^- and BF_4^- were observed. The silver atoms resulted in tetra- or pentacoordinated and no metal–metal interaction was present.

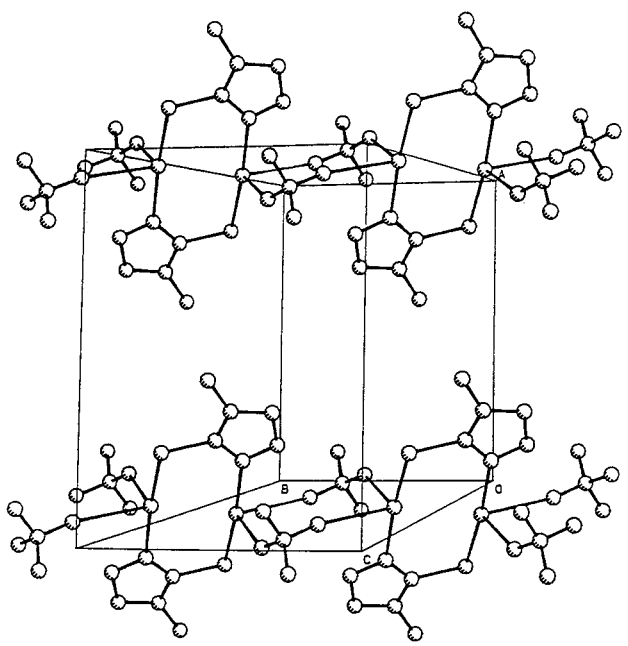

Fig. 4. Unit cell content of **II** showing rows of molecules joined by BF_4^- bridging anions to form infinite chains.

Table 4
Atomic coordinates and equivalent isotropic thermal parameters of complex **II** with estimated S.D. values in parentheses

	x/a	y/b	z/c	B_{eq}
Ag(1)	0.01360(6)	0.16472(8)	0.51763(3)	3.69(3)
P(1)	0.1758(2)	0.0783(3)	0.57287(8)	2.9(1)
N(1)	0.1463(6)	−0.2189(9)	0.5283(3)	3.1(3)
N(2)	0.2986(6)	−0.2192(9)	0.5865(3)	3.2(3)
C(1)	0.2092(7)	−0.132(1)	0.5635(3)	3.1(4)
C(2)	0.1978(8)	−0.368(1)	0.5286(4)	3.8(4)
C(3)	0.2918(8)	−0.368(1)	0.5642(3)	3.7(4)
C(4)	0.3913(8)	−0.164(1)	0.6257(4)	3.8(4)
C(5)	0.4440(8)	−0.297(1)	0.6582(3)	3.6(4)
C(6)	0.5620(8)	−0.318(1)	0.6614(4)	4.6(5)
C(7)	0.614(1)	−0.438(2)	0.6930(5)	6.7(7)
C(8)	0.546(1)	−0.532(2)	0.7224(4)	6.1(6)
C(9)	0.430(1)	−0.512(1)	0.7181(4)	6.0(6)
C(10)	0.380(1)	−0.394(1)	0.6868(4)	4.6(5)
C(11)	0.1544(7)	0.100(1)	0.6399(3)	3.3(4)
C(12)	0.1307(9)	−0.029(1)	0.6711(4)	4.3(5)
C(13)	0.106(1)	−0.001(2)	0.7210(4)	5.4(6)
C(14)	0.103(1)	0.148(2)	0.7396(4)	5.4(6)
C(15)	0.124(1)	0.278(2)	0.7096(5)	5.6(6)
C(16)	0.1495(8)	0.255(1)	0.6594(4)	4.1(5)
C(17)	0.3132(7)	0.179(1)	0.5638(3)	3.2(4)
C(18)	0.3954(8)	0.220(1)	0.6030(4)	3.5(4)
C(19)	0.4998(8)	0.286(1)	0.5932(4)	4.4(5)
C(20)	0.521(1)	0.311(1)	0.5441(6)	6.2(6)
C(21)	0.438(1)	0.273(2)	0.5038(5)	7.0(7)
C(22)	0.333(1)	0.207(1)	0.5131(4)	5.0(5)
F(1)	0.0981(7)	0.332(1)	0.4377(3)	7.3(5)
F(2)	0.0311(7)	0.572(1)	0.4239(3)	6.3(4)
F(3)	−0.021(1)	0.385(1)	0.3682(3)	8.7(5)
F(4)	0.158(1)	0.476(1)	0.3747(5)	9.1(8)
B(1)	0.074(2)	0.443(2)	0.4005(5)	7.0(8)
Cl(1)	0.7517(4)	0.1248(6)	0.6935(2)	9.8(3)
C(23)	0.830(1)	0.146(2)	0.6404(5)	9(1)
Cl(2)	0.8354(7)	−0.024(1)	0.6077(3)	8.1(5)

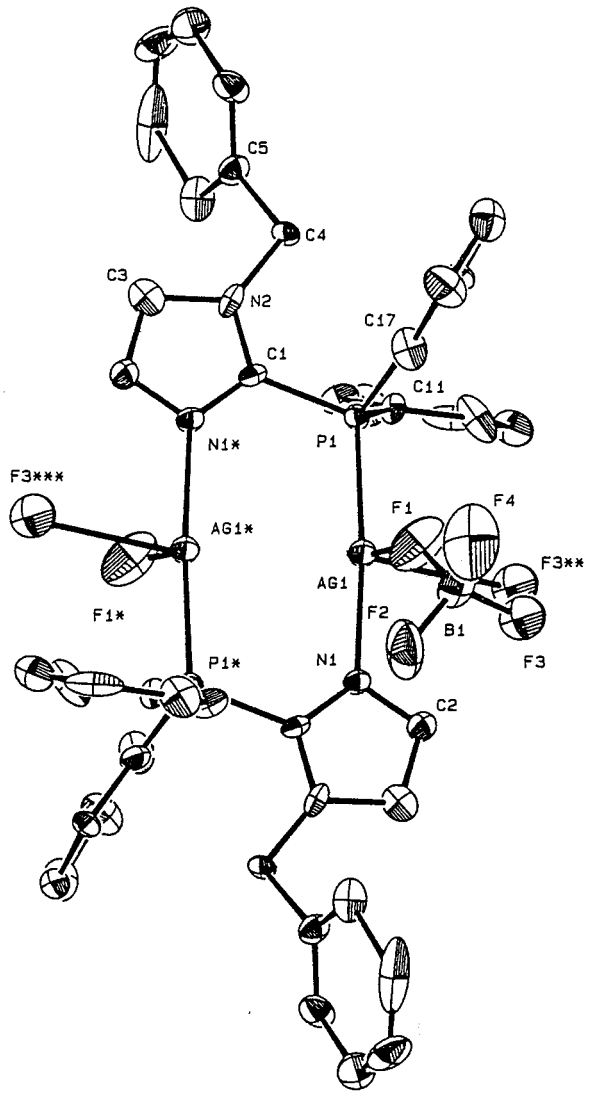

Fig. 5. ORTEP plot of **II** with the numbering schemes of the atoms. Atoms labeled with asterisks are centrosymmetric. Thermal ellipsoids are shown at 40% probability levels.

Table 5
Selected bond distances (Å) and angles (°) of complex **II**

Coordination sphere around Ag(1)	
Ag(1)···Ag(1′)	2.910(2)
Ag(1)···Ag(1″)	5.670(2)
Ag(1)–N(1)	2.148(7)
Ag(1)–P(1)	2.361(2)
Ag(1)–F(1)	2.779(8)
Ag(1)–F(3″)	2.756(8)
Ag(1′)···Ag(1)–P(1)	87.60(7)
Ag(1′)···Ag(1)–N(1)	87.8(2)
Ag(1′)···Ag(1)–F(1)	106.0(2)
Ag(1′)···Ag(1)–F(3″)	155.6(2)
N(1)–Ag(1)–P(1)	172.7(2)
N(1)–Ag(1)–F(1)	79.4(3)
N(1)–Ag(1)–F(3′)	86.8(3)
P(1)–Ag(1)–F(1)	107.4(2)
P(1)–Ag(1)–F(3′)	95.0(2)
F(3″)–Ag(1)–N(1)	141.3(2)
F(3″)–Ag(1)–F(1)	96.4(3)

In dichloromethane solution the cyclic $[\mu\text{-}(Bzim)Ph_2PAg]_2^{2+}$ unit is retained in all the complexes as demonstrated by the presence of the isotopomer patterns in ^{31}P-NMR spectra. Moreover, considering the NMR parameters recorded for complexes **I**–**III**, the cyclic dinuclear unit should be the unique species present in solution. The interionic structure in solution of the complex **II** determined by $^{19}F\{^1H\}$-HOESY NMR shows that the BF_4^- anion is not more coordinated to the silver(I) atoms as in the solid state, but it is localized in between the phenyl and benzyl groups of the ligand. On the other hand, considering the NMR parameters weak interactions with the metallic centers should be retained in solution.

As expected the $B[3,5\text{-}(CF_3)_2C_6H_3]^{4-}$ anion resulted in being the less interacting anion and this could be the reason for the minor stability of complex **III**, with

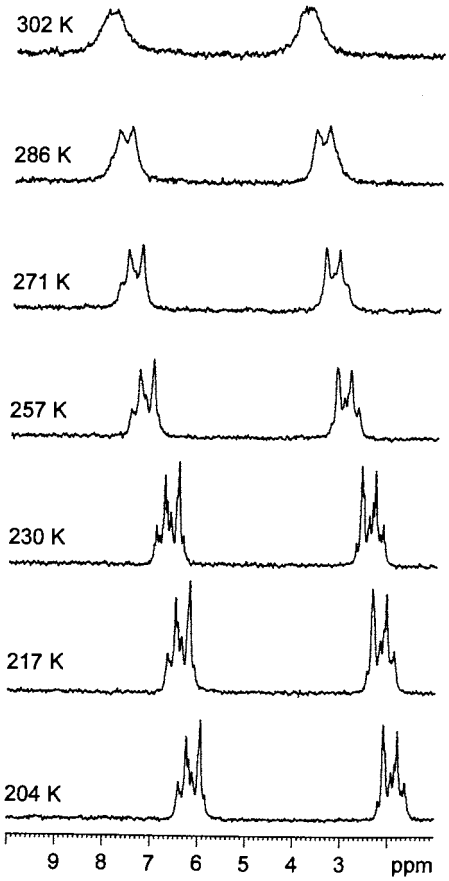

Fig. 6. Variable-temperature ^{31}P-NMR spectra of complex **II** recorded at 162 MHz in $(CD_3)_2CO$.

respect to the others, either in the solid state and in solution. The presence of small amount of the species $[\mu\text{-(Bzim)Ph}_2\text{P})_3\text{Ag}_2]^{2+}$ mixed to the complexes **I**–**III** evidenced by NMR spectroscopy could be indicative of ligand exchange between the cyclic units; further investigations are in progress and will be the object of a coming paper. Coordinating solvents could make these ligand exchanges easier and this could be the reason for the different ^{31}P-NMR pattern recorded in CD_3CN for compound **I** and **II** previously reported [14].

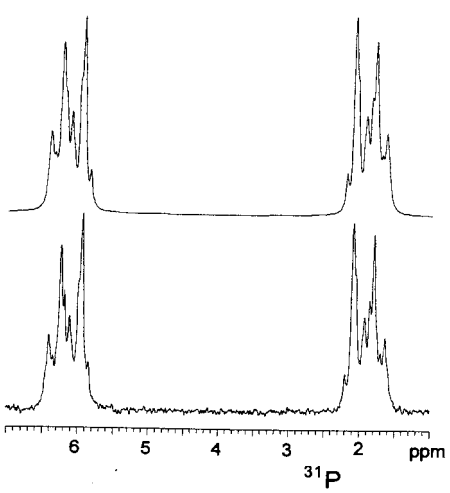

Fig. 7. Experimental and simulated ^{31}P-NMR spectra of complex **II** recorded at 162 MHz in CD_2Cl_2 at 217 K.

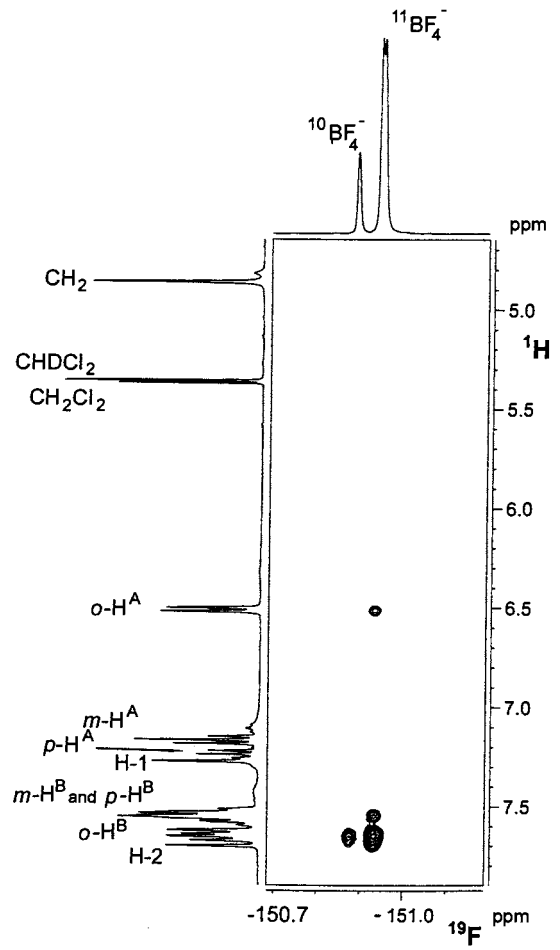

Fig. 8. Section of the ^{19}F{^{1}H}-HOESY spectrum of complexes **II** recorded at 376 MHz in CD_2Cl_2 at 217 K showing the interionic interactions of BF_4^- and the aromatic protons of the benzyl (A) and the *ortho* protons of the other phenyl groups (B) of the phosphine ligand.

4. Experimental

Elemental analyses were carried out on a Carlo Erba 1106 elemental microanalyzer. Infrared spectra were recorded in the range 4000–200 cm^{-1} on a Perkin–Elmer 1310 spectrophotometer using Nujol mulls in CsI windows. Compounds **I**, **II** [14] and $NaB[3,5\text{-}(CF_3)_2C_6H_3]_4$ [40] were prepared as described.

*4.1. Synthesis of complex **III** by metathesis of $[\mu\text{-(Bzim)Ph}_2\text{PAg}]_2[BF_4]_2$ with $NaB[3,5\text{-}(CF_3)_2C_6H_3]_4$*

The derivative **II** was dissolved in 6 ml of CH_3OH (0.04 g, 3.72×10^{-5} mol) and after dissolution

Table 6
^{31}P-NMR data for complexes **I–III**

	δ (ppm)	$^1J(^{31}P–^{107}Ag)$ (Hz)	$^1J(^{31}P–^{109}Ag)$ (Hz)	$^3J(^{31}P–^{107}Ag)$ (Hz)	$^3J(^{31}P–^{109}Ag)$ (Hz)	$^4J(^{31}P–^{31}P)$ (Hz)
NO_3^-	3.8	624	721	−14	−17	34
BF_4^-	4.0	637	735	−13	−15	25
BAr_4^-	6.7	638	736	−9	−11	17

$NaB[3,5\text{-}(CF_3)_2C_6H_3]_4$ (0.066 g, 7.44×10^{-5} mol) was added. After 3 h of magnetic stirring the colorless solution was pumped down to dryness. The crude product was extracted by $CHCl_3$ (4 ml). The analytical sample **III** was obtained by adding hexane (2 ml) and storing at 4°C.

Elemental analysis for $C_{108}H_{62}N_4P_2Ag_2B_2F_{48}$. Calc. C, 49.38; H, 2.38; N, 2.13. Found: C, 49.23; H, 2.28; N, 2.01%.

IR: 3150 (w), 2724 (w), 2670 (vw), 1610 (s), 1498 (w), 1354 (m), 1277.5 (s), 1078.7 (br, s), 994.9 (m), 924 (vw), 887.8 (m-w), 837.2 (m), 770.2 (m-w), 742.6 (m), 716.9 (s), 690.9 (m), 681.6 (m), 667.9 (m), 624 (m), 575.5 (m-w), 537.9 (m-w), 528 (m-w), 509 (m-w), 464 (w), 448.3 (m-w), 509.2 (m), 464.5 (m-w), 448.3 (m-w), 365.5 (w).

4.2. NMR investigation

One- and two-dimensional ^{1}H-, ^{13}C-, ^{19}F-, and ^{31}P-NMR spectra were measured on Bruker DPX 200 and DRX 400 spectrometers. Referencing is relative to TMS (^{1}H and ^{13}C), CCl_3F (^{19}F), and 85% H_3PO_4 (^{31}P). NMR samples were prepared by dissolving about 20 mg of compound in 0.5 ml of deuterated solvent. Two-dimensional ^{1}H-NOESY and $^{19}F\{^1H\}$-HOESY spectra were recorded with a mixing time of 500–800 ms.

4.2.1. Variable-temperature NMR experiments

In a typical experiment, approximately 20 mg of complex was dissolved in 0.6 ml of CD_2Cl_2 or $(CD_3)_2CO$. The ^{1}H-, ^{19}F- and ^{31}P-NMR spectra were recorded over the temperature range 204–302 K.

4.2.2. Characterization of complex *I*

^1H-NMR (CD_2Cl_2, 217 K): δ 7.49 (m, 22H, H-2, o-H^B, m-H^B and p-H^B), 7.23 (t, 2H, $^3J_{HH} = 7.3$, p-H^A), 7.16 (t, 4H, $^3J_{HH} = 7.7$, m-H^A), 7.14 (s, 2H, H-1), 6.53 (d, 4H, $^3J_{HH} = 7.3$, o-H^A), 4.80 (s, 4H, CH_2). $^{31}P\{^1H\}$-NMR (CD_2Cl_2): δ 3.8 (m).

4.2.3. Characterization of complex *II*

^1H-NMR (CD_2Cl_2, 217 K): δ 7.70 (s, 2H, H-2), 7.63 (m, 8H, o-H^B), 7.55 (m, 12H, m-H^B and p-H^B), 7.28 (s, 2H, H-1), 7.24 (tt, 2H, $^3J_{HH} = 7.3$, $^4J_{HH} = 2.1$, p-H^A), 7.17 (m, 4H, m-H^A), 6.51 (d, 4H, $^3J_{HH} = 7.3$, o-H^A), 4.86 (s, 4H, CH_2). $^{13}C\{^1H\}$-NMR (CD_2Cl_2): δ 138.95 (d, $^1J_{CP} = 63.6$, C^{ipso}), 133.30 (s, C-2), 132.97 (d, $^2J_{CP} = 15.4$, o-C^B), 132.89 (s, p-C^B), 130.51 (d, $^3J_{CP} = 10.4$, m-C^B), 130.19 (s, $C^{A\ ipso}$), 129.38 (s, m-C^A), 129.11 (s, p-C^A), 128.64 (s, C-2), 127.56 (s, o-C^A), 124.12 (d, $^1J_{CP} = 40.9$, $C^{B\ ipso}$), 53.00 (s, CH_2). $^{19}F\{^1H\}$-NMR (CD_2Cl_2): δ −150.89 (b, $^{10}BF_4^-$), −150.95 (b, $^{11}BF_4^-$). $^{31}P\{^1H\}$-NMR (CD_2Cl_2): δ 4.0 (m).

4.2.4. Characterization of complex *III*

^1H-NMR (CD_2Cl_2, 217 K): δ 7.76 (br, 16H, o-H^X), 7.56 (m, 30H, p-H^X, H-2, o-H^B, m-H^B and p-H^B), 7.35 (s, 2H, H-1), 7.26 (t, 2H, $^3J_{HH} = 7.4$, p-H^A), 7.17 (t, 4H, $^3J_{HH} = 7.2$, m-H^A), 6.52 (d, 4H, $^3J_{HH} = 7.2$, o-H^A), 4.79 (s, 4H, CH_2). $^{19}F\{^1H\}$-NMR (CD_2Cl_2): δ −62.93 (s). $^{31}P\{^1H\}$-NMR (CD_2Cl_2): δ 6.7 (m).

5. Supplementary material

Crystallographic data for the structures reported in this paper have been deposited with the Cambridge Crystallographic Data Centre as supplementary material and the reference numbers are: CCDC 132675 and CCDC 132676.

Acknowledgements

This work was supported by grants from the University of Camerino and from the Ministero dell'Università e della Ricerca Scientifica e Tecnologica (MURST, Rome, Italy), Programma di Rilevante Interesse Nazionale, Cofinanziamento 1998–9.

References

[1] C.A. Mc Auliffe, W. Levason, Phosphine, Arsine and Stibine Complexes of the Transition Elements, Elsevier, Amsterdam, 1979.
[2] R. Mason, D.W. Meek, Angew. Chem. Int. Ed. Engl. 17 (1978) 183.
[3] R.J. Lancashire, in: G.F. Wilkinson, R.D. Gillard, J.A. McCleverty (Eds.), Comprehensive Coordination Chemistry, vol. 5, Pergamon, Oxford, 1987, pp. 798–801.
[4] M. Camalli, F. Caruso, Inorg. Chim. Acta 144 (1988) 205.
[5] C.W. Liu, H. Pan, J.P. Fackler, Jr., G. Wu, E. Wasylishen, M. Shang, J. Chem. Soc. Dalton Trans. (1995) 3691.
[6] E.C. Alyea, G. Ferguson, A. Smogyvari, Inorg. Chem. 21 (1982) 1369.
[7] B.-K. Teo, J.C. Calabrese, Inorg. Chem. 51 (1976) 2467.
[8] M.R. Churchill, J. Donahue, F.J. Rotella, Inorg. Chem. 15 (1976) 2752.
[9] D.M. Ho, R. Bau, Inorg. Chem. 22 (1983) 4073.

[10] D. Perreault, M. Drouin, A. Michel, V.M. Miskowski, W.P. Schaefer, P.D. Harvey, Inorg. Chem. 31 (1992) 695.
[11] E.L. Muetterties, C.W. Alegranti, J. Am. Chem. Soc. 94 (1972) 6386.
[12] A. Del Zotto, P. Di Bernardo, M. Tolazzi, G. Tomat, P. Zanonato, J. Chem. Soc. Dalton Trans. (1993) 3009.
[13] A. Del Zotto, P. Di Bernardo, M. Tolazzi, P.L. Zanonato, J. Chem. Soc. Dalton Trans. (1999) 979.
[14] A. Burini, B.R. Pietroni, R. Galassi, G. Valle, S. Calogero, Inorg. Chim. Acta 229 (1995) 299.
[15] International Tables for X-ray Crystallography, vol. IV, Kynoch Press, Birmingham, UK, 1974.
[16] TEXAN-TEXRAY Structure Analysis Package, M.S.C., 1985.
[17] M.R. Rosenthal, J. Chem. Edu. 50 (1973) 331.
[18] F. Caruso, M. Camalli, H. Rimml, L.M. Venanzi, Inorg. Chem. 34 (1995) 673.
[19] P. Pyykkö, Chem. Rev. 97 (1997) 597.
[20] F.A. Cotton, X. Feng, M. Matusz, R. Poli, J. Am. Chem. Soc. 110 (1988) 7077.
[21] L. Pauling, The Nature of the Chemical Bond, third ed., Cornel University Press, Ithaca, NY, 1960.
[22] G.W. Eastland, M.A. Mazid, D.R. Russell, M.C.R. Symons, J. Chem. Soc. Dalton Trans. (1980) 1682.
[23] A. Del Zotto, P. Rigo, G. Nardin, Inorg. Chim. Acta 247 (1996) 183.
[24] N.W. Alcock, P. Moore, P.A. Lampe, K.F. Mok, J. Chem. Soc. Dalton Trans (1982) 207.
[25] A. Del Zotto, E. Zangrando, Inorg. Chim. Acta 277 (1988) 111.
[26] G.A. Ardizzoia, G. La Monica, A. Maspero, M. Moret, N. Masciocchi, Inorg. Chem. 36 (1997) 2321.
[27] R.A. Stein, C. Knobler, Inorg. Chem. 16 (1977) 242.
[28] M. Dartiguenave, Y. Dartiguenave, A. Mari, A. Guitard, M.J. Olivier, A.L. Beauchamp, Can. J. Chem. 66 (1988) 2386.
[29] H. Nakai, Bull. Chem. Soc. Jpn. 56 (1983) 1637.
[30] P.B. Hitchcock, M.F. Lappert, R.G. Taylor, J. Chem. Soc. Chem. Commun. (1984) 1082.
[31] WINDAISY, Version 4.05, Bruker.
[32] S. Attar, N.W. Alcock, G.A. Bowmaker, J.S. Frye, W.H. Bearden, J.H. Nelson, Inorg. Chem. 30 (1991) 4166.
[33] A.F.M.J. van der Ploeg, G. van Koten, Inorg. Chim. Acta 51 (1981) 225.
[34] G. Bellachioma, G. Cardaci, A. Macchioni, G. Reichenbach, S. Terenzi, Organometallics 15 (1996) 4349.
[35] A. Macchioni, G. Bellachioma, G. Cardaci, V. Gramlich, H. Ruegger, S. Terenzi, L.M. Venanzi, Organometallics 16 (1997) 2139.
[36] A. Macchioni, G. Bellachioma, G. Cardaci, G. Cruciani, E. Foresti, P. Sabatino, C. Zuccaccia, Organometallics 17 (1998) 5549.
[37] G. Bellachioma, G. Cardaci, V. Gramlich, A. Macchioni, M. Valentini, C. Zuccaccia, Organometallics 17 (1988) 5025.
[38] C. Zuccaccia, G. Bellachioma, G. Cardaci, A. Macchioni, Organometallics 18 (1999) 1.
[39] A. Macchioni, G. Bellachioma, G. Cardaci, M. Travaglia, C. Zuccaccia, B. Milani, G. Corso, E. Zangrando, G. Mestroni, C. Carfagna, M. Formica, Organometallics 18 (1999) 3061.
[40] M. Brookhart, B. Grant, A.F.J. Volpe, Organometallics 11 (1992) 3920.